International Journal of Multiphase Flow 35 (2009) 597–600

Contents lists available at ScienceDirect

International Journal of Multiphase Flow

journal homepage: www.elsevier.com/locate/ijmulflow

Brief Communication

Threshold for sediment erosion in pipe flow

Y. Peysson [a,*], M. Ouriemi [b,c], M. Medale [c], P. Aussillous [c], É. Guazzelli [c]

[a] IFP, 1 et 4 Avenue de Bois-Préau, 92852 Rueil-Malmaison Cedex, France
[b] IFP-Lyon, Rond-Point de l'échangeur de Solaize, BP 3, 69360 Solaize, France
[c] IUSTI CNRS UMR 6595 – Polytech' Marseille – Aix-Marseille Université (U1), 5 rue Enrico Fermi, 13453 Marseille Cedex 13, France

ARTICLE INFO

Article history:
Received 22 December 2008
Received in revised form 28 January 2009
Accepted 10 February 2009
Available online 26 February 2009

Keywords:
Shields number
Sediment transport
Pipe flow

1. Introduction

The response of a sedimented bed of particles to shearing flows is an issue which has been widely studied and discussed for over a century. This problem is indeed at the center of the understanding of a variety of natural phenomena such as sediment transport in rivers and estuaries, erosion and deposition leading to the evolution of mountains and landscapes, and dune formation in the desert (aeolian dunes) or underwater. It is also of fundamental importance in numerous industrial processes such as slurry transport or cutting discharge by hydraulic transport in the mining industry. In practice, slurries which consist of mixtures of solid and fluid are conveyed through pipelines, see e.g. Matoušek (2005). Understanding the flow of settling slurries in pipelines is also of great interest in the oil and gas industry especially in the context of hydrate (solid crystal of clathrate) formation that are encountered in offshore oil production.

One of the essential issue in slurry transport is to predict the onset of solid flow. The usual way of representing the incipient motion of the particles is to use a dimensionless number called the Shields number, $\theta = \tau_b/(\rho_p - \rho_f)gd$, which measures the relative importance of the destabilizing hydrodynamic force, i.e. $\tau_b d^2$ where τ_b is the shear stress at the bed surface, and the stabilizing gravity force, i.e. the apparent weight of a grain $(\rho_p - \rho_f)d^3 g$, where d is the grain diameter, ρ_p and ρ_f the density of the solid and the fluid respectively, and g the acceleration due to gravity. The data, which are mostly collected in the turbulent flow regime as shown in e.g. White (1970), Mantz (1977), Yalin and Karahan (1979) and Dancey and Diplas (2002), are conventionally represented using the Shields curve by plotting θ against the boundary Reynolds number defined with the friction velocity $= \sqrt{\tau_b/\rho_f}$ as a velocity scale and d as length scale. This representation, which seems somehow circular, stems from Shields assumption that his measured shear stress attains a constant value for large Reynolds numbers which is based on analogy with Nikuradse (1933) finding that the friction factor (or drag coefficient) also reaches a constant value, see e.g. Buffington (1999) discussion of the Shields curve (his Fig. 4).

The main issue comes from unambiguously defining the shear stress τ_b. In the low-Reynolds-number viscous regime, it is defined as $\tau_b = \eta\dot{\gamma}$ where η is the fluid viscosity and $\dot{\gamma}$ the shear rate. In viscous pipe flow, Ouriemi et al. (2007) precisely computed this shear rate and, through measurement for the onset of grain motion, inferred a critical Shields number $\theta^c = 0.12$ independent of the Reynolds number for a large range of small particle Reynolds numbers. The objective of the present brief communication is to extend this approach up to the turbulent regime. In Section 2, the threshold for motion is characterized in a precise way through the cessation of granular motion. In Section 3, we propose a simple model in which the basic assumption is that the critical Shields number found in the laminar regime holds up to the turbulent regime. The shear stress is defined using the friction factor in the two limits of laminar and turbulent flows. In Section 4, this model is tested against the experiments.

2. Experiments

Four different batches of spheres and four mixtures of UCON oil 75H-90000 and water at different temperatures were used in the experiments, see their characteristics in Tables 1 and 2. The

* Corresponding author. Tel.: +33 147526960; fax: +33 147527002.
E-mail address: yannick.peysson@ifp.fr (Y. Peysson).

0301-9322/$ - see front matter
doi:10.1016/j.ijmultiphaseflow.2009.02.007

Table 1
Particle characteristics: diameter d and density ρ_p.

Batch	Composition	d (μm)	ρ_p (g/cm^3)
A	Glass	132 ± 22	2.490 ± 0.003
B	Polystyrene	538 ± 24	1.051 ± 0.002
C	PMMA	132 ± 20	1.177 ± 0.002
D	PMMA	193 ± 30	1.177 ± 0.002

Table 2
Fluid characteristics: viscosity η and density ρ_f.

Fluid	% UCON	T (°C)	η (cP)	ρ_f (g/cm^3)
1	0	20	1.00 ± 0.05	1.004 ± 0.001
2	0	35	0.70 ± 0.04	0.999 ± 0.001
3	12	35	8.8 ± 0.4	1.023 ± 0.001
4	20	35	40 ± 2	1.040 ± 0.001

experimental test section was a horizontal glass tube having a length 1.8 m and inner diameter $D = 3$ cm. Particles were introduced in the tube previously filled with the fluid to build a uniform flat bed of a given initial height. A constant flow rate was then imposed by gravitational overflow from an overhead tank and measured with a flowmeter with an accuracy of 3.2%. At the outlet of the tube, the particles were captured by a mesh while the fluid was run into a reservoir and then pumped back to the overflowing tank. Note that the captured particles were not re-injected into the tube. The bed was illuminated by a laser sheet aligned with the tube length. The illuminated upper layer of particles intersecting the sheet was imaged by a digital camera. After calibration, this provided a measurement of the bed height with an accuracy of 0.8 mm. Further details on the experimental techniques can be found in Ouriemi et al. (2007).

The critical flow rate for sediment erosion was characterized through the cessation of motion. When the flow rate was switched on for a given bed height, the particles started to be eroded from the bed surface. This caused the fluid height to increase and therefore the shear stress on the bed to decrease. The erosion eventually stopped when the shear stress reached a critical value. At that point, the bed had reached a rest height h which depended upon the constant imposed flow rate Q. This cessation of erosion corresponded precisely to the threshold of motion as by increasing the flow rate by a small amount particles were set again in motion.

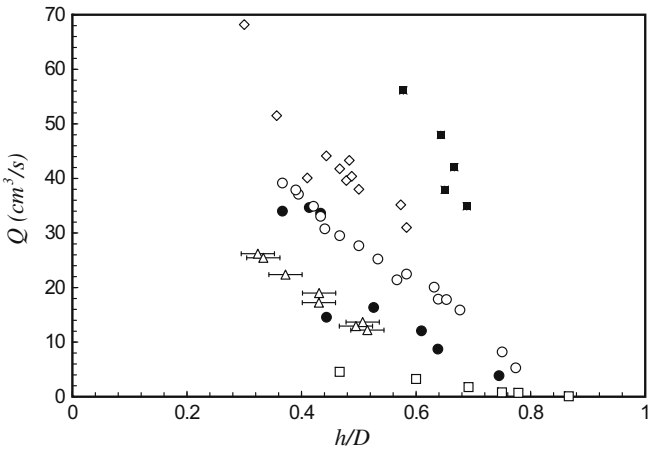

Fig. 1. Critical flow rate Q versus normalized bed height h/D for batch A in fluid 1 (■), batch A in fluid 3 (●), batch A in fluid 4 (○), batch B in fluid 2 (□), batch C in fluid 1 (△), and batch D in fluid 2 (◇). The error bars are only indicated for batch C in fluid 1 (△). Note that the vertical error bars are smaller than the size of the symbol.

In other words, there was no observed hysteresis between the threshold for motion and that for cessation of motion. Fig. 1 shows the flow rate versus the rest bed height h normalized by the pipe inner diameter D for different combination of fluid and particles. A clear decrease of the critical flow rate is observed when increasing the bed height in all experiments.

3. Model

The basic assumption is that there is a critical Shields number $\theta^c = \tau_b^c/(\rho_p - \rho_f)gd$ which characterizes the threshold for grain motion and that this criterion holds for both laminar and inertial flow regimes. The main difficulty lies in finding a proper definition of the shear stress τ_b at the top of the bed which remains valid throughout both regimes in the pipe geometry considered in the present study.

In a pipe of inner diameter D partially filled by a flat granular bed of height h, dimensional analysis gives

$$\tau_b = \frac{1}{2}\rho_f \left(\frac{Q}{S}\right)^2 f\left(Re, \frac{h}{D}\right), \tag{1}$$

where f is a dimensionless function which depends upon both the Reynolds number $Re = \rho_f DQ/\eta S$ and the filling fraction h/D whereas it is only controlled by Re in the pipe with no particles. Here, the Reynolds number is defined using the superficial velocity Q/S where Q is the flow rate and S the fluid section. The fluid section can be easily evaluated as $S/S_0 = \{2\arccos(1-2h/D) - 2(1-2h/D)\sin[\arccos(1-2h/D)]\}/2\pi$ using a simple geometrical calculation and $S_0 = \pi D^2/4$ being the pipe section. The Newtonian fluid has a density ρ_f and a viscosity η.

A classical approach is to consider that the pipe friction factor mainly depends upon a single dimensionless number instead of two, i.e. $f(Re, h/D) = f(Re_*)$, by using a new Reynolds number $Re_* = \rho_f D_* Q/\eta S$ built with a new length scale called the equivalent diameter D_*. This new diameter has been computed numerically in the viscous regime limit. In this limit, the incompressible Navier–Stokes equations reduce to the Stokes equations as there is only a single non-zero component of the velocity along the pipe length. These equations have been solved with a no-slip boundary condition along the wetted perimeter and an imposed flow rate. This yields the calculated shear stress at the top of the bed which is assumed to be equivalent to that for a pipe with no particles having an inner diameter D_*, i.e. $\tau_b(h/D) = 8\eta Q/SD_*$. Therefore, $D_*/D = S_0\tau_b(h/D=0)/S\tau_b(h/D)$ can be directly computed, see Fig. 2. Note that D_* differs from the classical hydraulic diameter defined as $D_h = 4S/P$ where P is the wetted perimeter (also plotted for comparison in Fig. 2).

Using the above definition of the shear stress at the top of the bed, we rewrite the threshold for grain motion, $\theta^c = (\rho_f Q^{c2}/2S^2)\, f(Re_*^c)/(\rho_p - \rho_f)gd$ where the superscript c indicates that the quantities are evaluated at threshold, as

$$\left(\frac{Q^c}{Q_0}\right)^2 = \frac{2\theta^c\left(\frac{S}{S_0}\right)^2}{f(Re_*^c)} = \frac{2\theta^c\left(\frac{S}{S_0}\right)^2}{f\left(\frac{Q^c}{Q_0}\frac{D_*}{D}\frac{S_0}{S}Re_0\right)}, \tag{2}$$

where $Q_0 = U_0 S_0$ and $Re_0 = \rho U_0 D/\eta$ are respectively a flow rate and Reynolds number in the open pipe of inner diameter D and section $S_0 = \pi D^2/4$ based on a velocity $U_0 = \sqrt{(\rho_p - \rho_f)gd/\rho_f}$. Note that the significance of U_0 can be derived from the same balance that gives the Shields number if one assumes that $\theta^c \sim 1$ and $\tau_b = \rho_f U_0^2$.

The friction factor of a pipe $f(Re_*)$ is well known in the Stokes regime and is given by

$$f(Re_*) = \frac{16}{Re_*}. \tag{3}$$

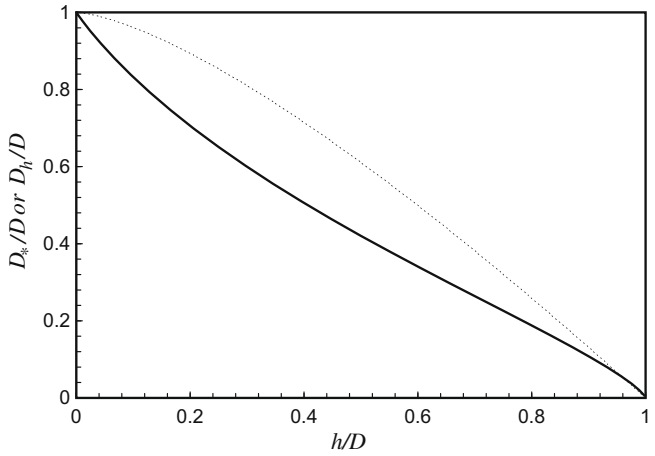

Fig. 2. Normalized equivalent diameter D_*/D (solid line) and hydraulic diameter D_h/D (dotted line) versus filling fraction h/D.

In the turbulent regime at large Re_*, i.e. $Re_* \gtrsim 10^4$, the roughness of the wall ϵ needs to be accounted in the present case of a granular bed since it has an effect on the boundary layer and thus influences the friction factor. By dimensional analysis, the roughness effect comes about through its relative dimension to that of the pipe, i.e. ϵ/D_*. Comprehensive studies of turbulent flow in pipes of well defined roughness were performed by Nikuradse (1933) who found the empirical correlation

$$\frac{1}{\sqrt{f}} = 4\log\left(\frac{D_*}{2\epsilon}\right) + 3.48. \tag{4}$$

In between these two limiting regimes, one can find numerous useful correlations, see e.g. chapter 4 of Govier and Aziz (1972) and chapter 1 of Shook and Roco (1991), among which that of Churchill (1977) meant to be valid in all regimes

$$f = 2\left[\left(\frac{8}{Re_*}\right)^{12} + (A+B)^{-1.5}\right]^{1/12} \quad \text{where}$$

$$A = \left\{-2.457\ln\left[\left(\frac{7}{Re_*}\right)^{0.9} + \frac{0.27\epsilon}{D_*}\right]\right\}^{16} \quad \text{and}$$

$$B = \left(\frac{37530}{Re_*}\right)^{16}, \tag{5}$$

see Fig. 3.

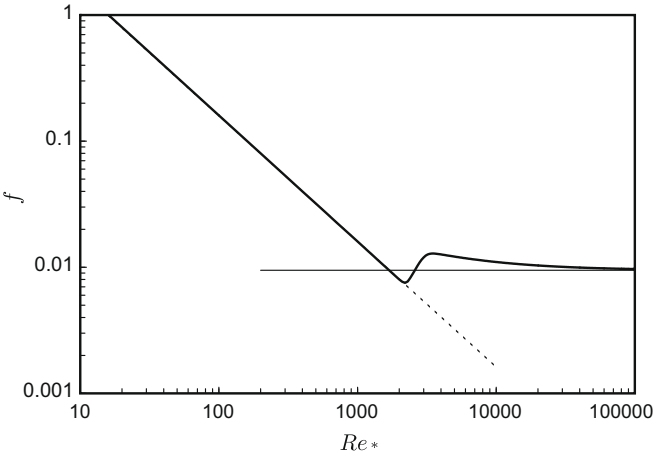

Fig. 3. Friction factor f versus Reynolds number Re_* for $\epsilon/D_* = 0.01$: Stokes formula (3) (dotted line), Nikuradse (1933) correlation (4) (thin solid line), and Churchill (1977) correlation (5) (thick solid line).

4. Comparison and conclusion

Eq. (2) is solved using the different expressions for the friction factor introduced in Section 3 and is tested in Fig. 4 against the experiments presented in Section 2 using $\theta^c = 0.12$ and D_* given in Fig. 2 found in the viscous regime. The Reynolds number $Re_0 = \rho U_0 D/\eta$ is computed by using the fluid and particles properties for each data set.

The inertial and laminar regimes present a different qualitative trend of the data. The Stokes friction factor provides a good approximation up to large Re_0, see the comparison between the model and the experimental observations for $Re_0 = 33$ (○), 150 (●), and 440 (△). The Nikuradse (1933) correlation, which gives an upper bound for large Reynolds numbers, agrees well with the experimental data at $Re_0 = 1870$ (■) with $\epsilon/D_* = 0.01$. In the present experiments, $0.004 \lesssim d/D \lesssim 0.017$ (see Table 1) are of the same order of magnitude as $\epsilon/D_* = 0.01$. Therefore, the effective roughness, i.e. the roughness in the equivalent pipe with no particles of diameter D_*, seems to be determined by the particle size d. However, note that f has a weak variation with ϵ/D_* in the Nikuradse (1933) correlation (4). The Churchill (1977) correlation also gives a good agreement with $\epsilon/D_* = d/D = 0.004$ for batch A at $Re_0 = 1870$ since this correlation hold for all regimes.

In the intermediate regime where the transition from laminar to turbulent flows takes place, the Churchill (1977) correlation yields a good estimate with $\epsilon/D_* = d/D = 0.017$ for batch B at $Re_0 = 710$ (□) and $\epsilon/D_* = d/D = 0.006$ for batch D at $Re_0 = 820$ (◇). Interestingly, the Nikuradse (1933) correlation provides a decent agreement too since f presents a very slow decrease with Re_* for these intermediate Reynolds numbers, see Fig. 3. Note that the data are more scattered in this transition regime. This may be due to the nature of the transition. Indeed, the transition happens to be subcritical and therefore is very sensitive to finite amplitude perturbations. Localised disturbances at the level of the pipe (which can include surface roughness or local constriction of the pipe) as well as suspended particles have been observed to influence strongly the transition, see e.g. Darbyshire and Mullin (1995), Matas et al. (2003), and Peixinho and Mullin (2007).

In summary, the two limits of Stokes and Nikuradse frictions seems to be able to describe incipient motion for all fluid-flow regimes using a classical equivalent-pipe approach and assuming a

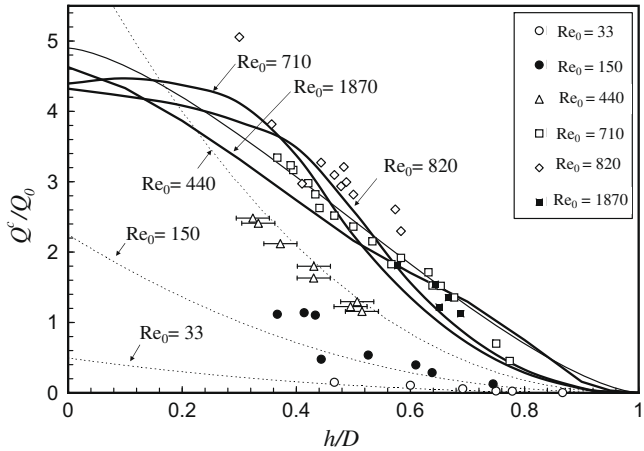

Fig. 4. Normalized flow rate Q^c/Q_0 versus filling fraction h/D. The symbols correspond to the experiments shown in Fig. 1 and the lines to the resolution of Eq. (2) using for the friction factor the Stokes formula (3) (dotted line), the Nikuradse (1933) correlation (4) (thin solid line), and the Churchill (1977) correlation (5) (thick solid line) as well as $\theta^c = 0.12$ and D_* given in Fig. 2. The Reynolds number Re_0 is computed by using the fluid and particles properties for each data set. The error bars are only indicated for batch C in fluid 1 (△).

constant critical Shields number. This latter assumption will prevail until lift forces become dominant for much higher Reynolds numbers, typically $Re \gtrsim 10^6$, see e.g. Mollinger and Nieuwstadt (1996) and references wherein.

References

Buffington, J.M., 1999. The legend of A.F. Shields. J. Hydraulic Eng. 125, 376–387.

Churchill, S.W.J., 1977. Friction factor equation spans all fluid-flow regimes. Chem. Eng. 84, 91–92.

Dancey, C.L., Diplas, A.N., 2002. Probability of individual grains movement and threshold condition. J. Hydr. Eng. 128, 12.

Darbyshire, A.G., Mullin, T., 1995. Transition to turbulence in constant-mass-flux pipe flow. J. Fluid Mech. 289, 83–114.

Govier, G.W., Aziz, K., 1972. The Flow of Complex Mixture in Pipes. Van Nostrand Reinhold Company, New York.

Mantz, P.A., 1977. Incipient transport of fine grains and flanks by fluids-extended Shields diagram. J. Hydr. Div. 103, 601.

Matas, J.P., Morris, J.F., Guazzelli, E., 2003. Transition to turbulence in particulate pipe flow. Phys. Rev. Lett. 90, 014501.

Matoušek, V., 2005. Research developments in pipeline transport of settling slurries. Powder Technol. 156, 43–51.

Mollinger, A.M., Nieuwstadt, F.T.M., 1996. Measurement of the lift force on a particle fixed to the wall in the viscous sublayer of a fully developed turbulent boundary. J. Fluid Mech. 316, 285–306.

Nikuradse, J., 1933. Strömungsgesetze in rauhen Rohren. Forshungsheft 361. V.D.I. Verlag, Berlin, 22 pp.

Ouriemi, M., Aussillous, P., Medale, M., Peysson, Y., Guazzelli, E., 2007. Determination of the critical Shields number for particle erosion in laminar flow. Phys. Fluids 19, 061706.

Peixinho, J., Mullin, T., 2007. Finite-amplitude thresholds for transition in pipe flow. J. Fluid Mech. 582, 169–178.

Shook, C.A., Roco, M.C., 1991. Slurry Flow: Principles and Practice. Butterworth–Heinemann Series in Chemical Engineering, Stoneham.

White, S.J., 1970. Plane bed thresholds of fine grained sediment. Nature 228, 152.

Yalin, M.S., Karahan, E., 1979. Inception of sediment transport. J. Hydr. Div. 105, 1433.